# SELF-ORGANIZING
## STRUCTURES AND NANOASSEMBLIES

# Photoconductivity of a Composite of Poly-N-Vinylcarbazole with Carbocyanine Dye Increased by Silicon Nanoparticles

**A. V. Astafev**[a,*,**], **I. R. Sayarov**[b], **M. G. Tedoradze**[b], **A. S. Ilin**[c], and **A. R. Tameev**[a,b]

[a] *Tikhonov Moscow Institute of Electronics and Mathematics,*
*National Research University Higher School of Economics, Moscow, 101000 Russia*
[b] *Frumkin Institute of Physical Chemistry and Electrochemistry, Russian Academy of Sciences, Moscow, 119071 Russia*
[c] *Faculty of Physics, Lomonosov Moscow State University, Moscow, 119991 Russia*
*\*e-mail: avastafev@gmail.com*
*\*\*e-mail: aastafev@hse.ru*

**Abstract**—Photoconductivity of a composite of poly-N-vinylcarbazole with carbocyanine dye was studied. The efficiency of photogeneration of charge carriers was measured by the electrographic discharge technique. The photocurrent in composite films increased when a hole transport layer was deposited on electrode and n-type silicon nanoparticles were incorporated into the layer. The Si nanoparticles can serve as additional hole transport pathways and increase the efficiency of the photogeneration of charge carriers in the photoconductor composite.

## INTRODUCTION

Photoconductivity is determined by two key processes: the photogeneration of free charge carriers and their transport in the photoconductor. The electrographic (EG) method allows one to measure the photogeneration quantum efficiency (PQE) of free electrons and holes in a photoconductor deposited onto electrode. The method is based on the forming a double electric layer in a photoconductor film when monopolar ions are deposited on its top surface [1, 2]. The ions are created by the corona discharge and form a potential $V_0$ above the film relative to the grounded counter electrode. The electric field strength that arises in the film serves as the driving force for the photogeneration of charge carriers and the subsequent drift of monopolar charge carriers to the electrode leading to neutralization of the surface charge or to a decrease in the thickness of the electrical double layer. When the film is illuminated, a decrease in the surface potential V is recorded.

The advantage of the EG method compared to the method of measuring photoconductivity in diode structure is that no ohmic contacts are needed. The formation of ohmic contacts is difficult to implement, for example, for new materials with unknown values of the energy levels of frontier molecular orbitals and the Fermi level.

The PQE is also measured using the time-of-flight technique as described for two π-conjugated polymers [3]. Specimens are as a thin film diode and one electrode (ITO) is transparent to the light pulse. In this method of the PQE measurements, the result depends on the nature of the charge carrier capture in deep traps, diffusion drift transport. The EG method is less sensitive to the influence of the charge carrier transport nature, since the main contribution to the recording signal is made by the initial shift of charge carriers before their capture in deep traps.

The PQE is also determined by measuring the short circuit current in a diode exhibiting the photovoltaic effect [4]. This approach is not suitable for studying the dependence of the PQE on the electric field.

Conventional poly-N-vinylcarbazole (PVC) is well suited for studying the photoconductivity of a polymer semiconductor and its sensitization to a given spectral range [5]. PVC possesses mobile holes [6], its films can be easily prepared from solution at room temperature, so the polymer is used as a hole transport layer (HTL) for perovskite solar cells [7, 8].

The purpose of this work is to study the possibility of increasing the photocurrent and PQE of charge carriers in films of a photoconductive PVC composite with a carbocyanine dye. An increase in the efficiency of hole transfer from the composite film to the ITO electrode is achieved by introducing an HTL based on
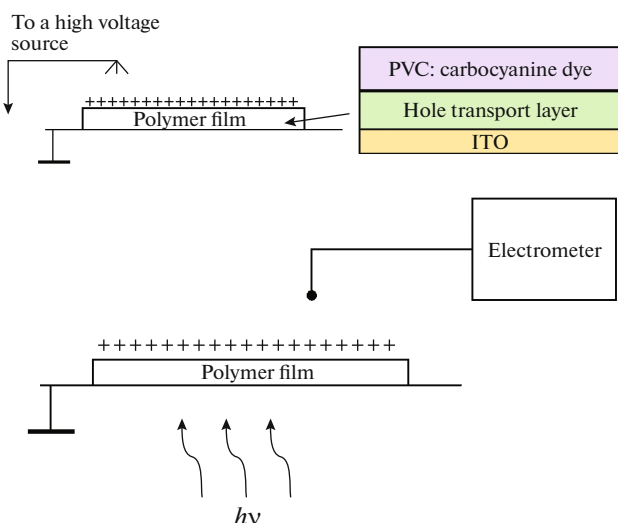
**Fig. 1.** Scheme of (a) charging the surface of a polymer film with ions and (b) measuring the surface potential.

the polymer semiconductor PEDOT. In addition, the HTL is doped with silicon nanoparticles to increase its conductivity.

## EXPERIMENTAL SETUP

Charging the film surface, i.e. the deposition of ions, is carried out as follows (Fig. 1). An electric

potential of 5−7 kV relative to ground is applied to thin wires (the substrate with the applied film is grounded) to generate a corona discharge in air. The grid between the specimen and the corona wires is at a potential in the range of 200−500 V, the same polarity as the corona wires, and directs ions of the same polarity ($O_3^-$ or $H_2O^+$) onto the specimen. A potential difference arises between the film surface and the grounded substrate. When the specimen is illuminated, the absorbed photons generate electrons and holes in the photoconductor film. Charge carriers with the same sign as surface ions drift towards the grounded substrate, and charge carriers with the opposite sign remain in the bulk or drift towards the surface of the film and compensate the charge of the surface ions. In this case, the potential above the film surface decreases. A scheme of the experimental setup for recording the kinetics of the decay of the potential $V(t)$ on the film surface is shown in Fig. 2. To record the potential V above the film surface, an electrometer based on a field-effect transistor was assembled in an EG setup. This design of the device allows us to adjust the sensitivity of the measuring probe using a variable resistance in the RC circuit. Figure 3 shows the electrical circuit of the measuring part. The electrometer consists of a KP303B field-effect transistor, two resistances 1 and 50 kΩ, and an electrical capacitance (neon lamp). The acquisition of recorded signals is carried out using an analog-to-digital converter
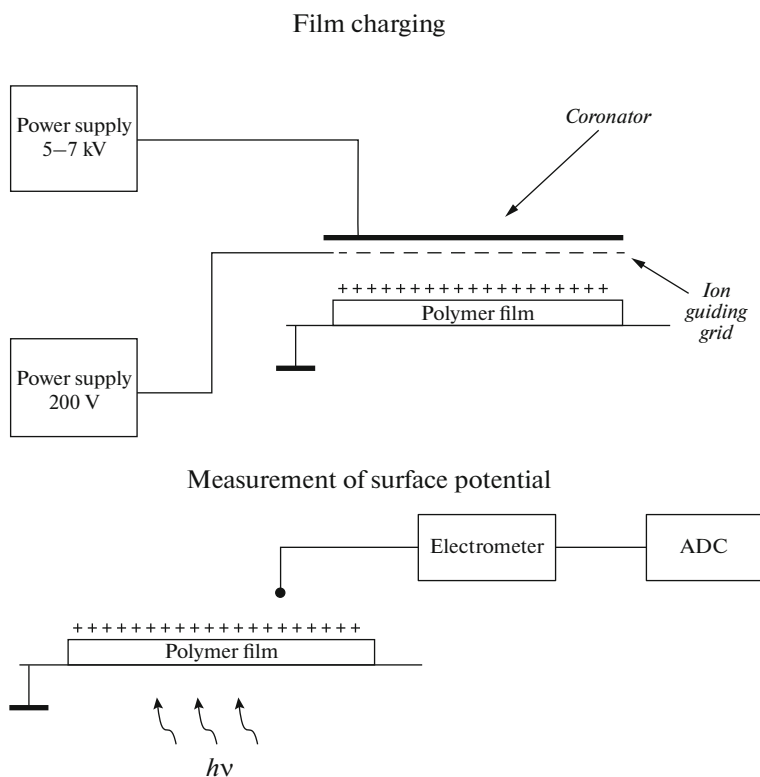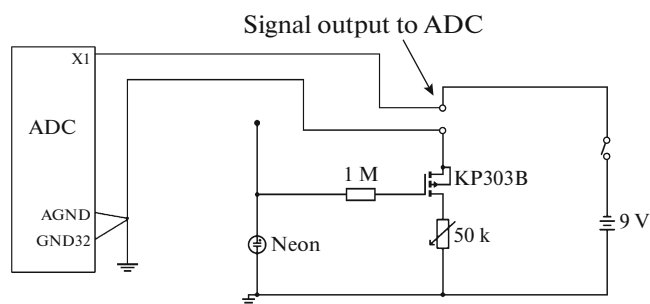


**Fig. 2.** Experimental setup.

Fig. 3. Electrical circuit of the measuring part.

(ADC) connected in single-phase mode with a common ground. The choice of ADC is determined by the input signal ranges $\pm10$, $\pm2.5$, $\pm0.625$, $\pm0.156$ V, its synchronization pulse to trigger recording, sampling frequency of ~360−400 Hz, measurement error $\pm0.05\%$, and the ability to directly export data to graphics packages.

## MATERIALS AND SPECIMENS

Structures of (a) complex of poly(3,4-ethylenedioxythiophene) with polystyrene sulfonic acid (PEDOT:PSS, Clevios AI 4083), (b) poly-N-vinylcarbazole (PVC, Acros) and (c) 1,1'-dimethyl-3,3'-tetramethylcarbocyanine perchlorate dye (CD, EPFL) are presented in Fig. 4. For electrical testing, specimens of the glass/ITO/PEDOT:PSS/PVC:CD structure were prepared, where a layer of PEDOT:PSS and a layer of the photoactive PVC:CD composite were sequentially deposited onto a glass substrate with a transparent conductive ITO layer. A 40 nm thick PEDOT:PSS layer was prepared from an aqueous solution by the spin coating method; the layer served
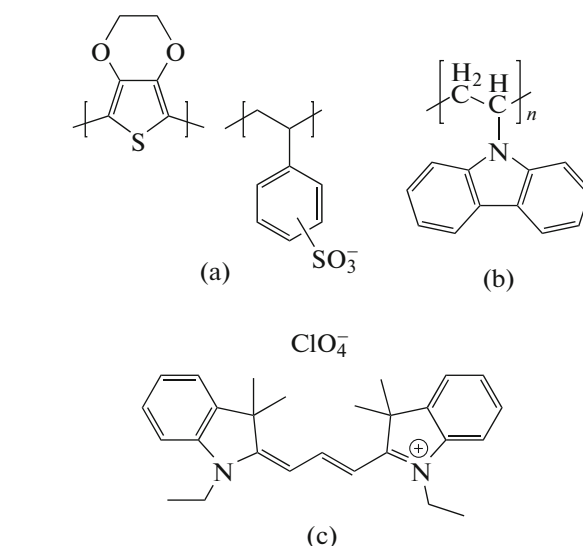


Fig. 4. Structure of (a) poly(3,4-ethylenedioxythiophene) polystyrene sulfonate (PEDOT:PSS), (b) poly-N-vinyl-carbazole (PVC), and (c) 1,1'-dimethyl-3,3'-tetramethyl-carbocyanine perchlorate dye (CD).

as an HTL that ensured the transport of holes from the photoactive layer to the ITO electrode. ITO/glass substrates coated with PEDOT:PSS were calcined in a thermal chamber at a temperature of 90°C for 15 minutes and slowly cooled to room temperature. Silicon nanoparticles with an average size of 80 nm were obtained by laser ablation of a silicon wafer [9]. To form a polymer composite, PVC with a molecular weight of 90.000 was dissolved in chlorobenzene (100 mg/mL) and CD was added at a concentration of 0.5 mg/mL. The solution was stirred for 24 h. Then the solution of the PVC:CD composite was drop cast to
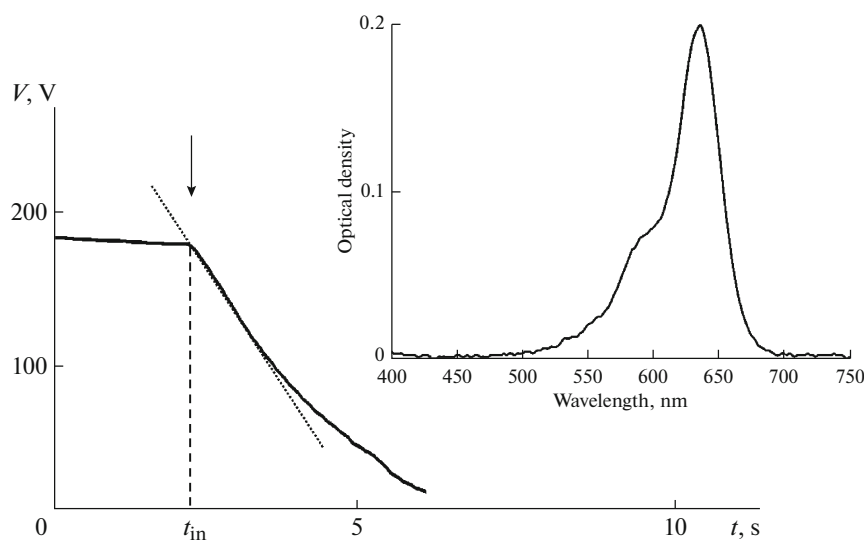


Fig. 5. Potential decay curve $V(t)$ of a specimen with a PEDOT:PSS HTL with Si nanoparticles. The arrow shows the turning on the illumination. The inset shows the absorption spectrum of the PVC:CD composite film.
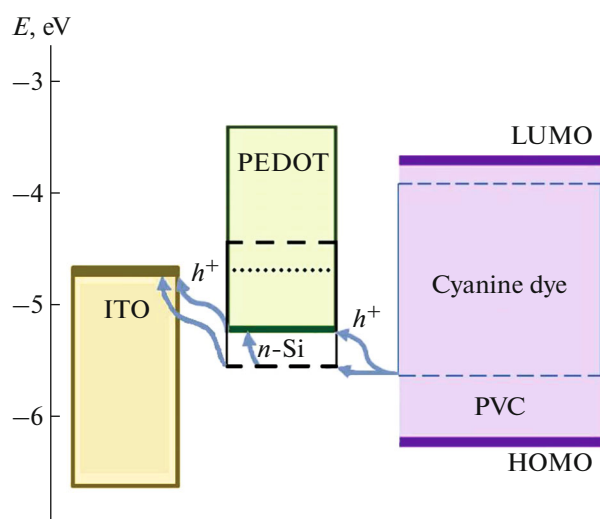
**Fig. 6.** Energy diagram of the highest occupied molecular orbital (HOMO) and lowest unoccupied molecular orbital (LUMO) for organic molecules, conductive and valence bands of Si and the work function of ITO relative to vacuum level [10].

the glass/ITO/PEDOT:PSS substrate and dried in a closed dish with chlorobenzene vapor for 24 h to slowly remove the solvent. As a result, a homogeneous film with a thickness of 2.5 μm was obtained. The absorption spectrum of the PVC:CD composite film is shown in Fig. 5.

## RESULTS AND DISCUSSION

The external PQE Φ was calculated using the following relation

$$\Phi = C \times \left(\frac{dV}{dt}\right)_0 \times \frac{E_{\text{ph}}}{e \times P_{\text{in}} \times \left(1 - 10^{-D}\right)}, \qquad (1)$$

where $C$—specific electrical capacitance of a polymer film [F/cm²], $(dV/dt)_0$—rate of potential decay at the initial moment of illumination [V/s], $P_{\text{in}}$—incident light power [W/cm²], $D$—optical density of the composite film, $E_{\text{ph}}$—photon energy [J], $e$—electron charge [C]. For a specimen with a PEDOT:PSS HTL containing Si nanoparticles, the surface potential decay when exposure by light with a wavelength of 620 nm is shown as an example in Fig. 6. Similar

**Table 1.** Initial rate of the surface potential decay and PGE in specimens with different hole transport layer (HTL)

| HTL in specimens | No HTL | PEDOT:PSS | PEDOT:PSS with Si nanoparticles |
|---|---|---|---|
| $(dV/dt)_0$, V/s | 14.8 ± 1.0 | 28.4 ± 2.0 | 36.0 ± 3.5 |
| PGE, % | 1.3 ± 0.1 | 1.8 ± 0.1 | 3.3 ± 0.3 |

curves were recorded for specimens with HTL made of only PEDOT:PSS and HTL free specimens. The measurement results and the obtained external PQE values are presented in Table 1.

In specimens with HTL containing Si nanoparticles, the nanoparticles penetrate into the photoactive layer since the size of Si nanoparticles (80 nm) exceeds the thickness of the PEDOT:PSA layer (40 nm). The increased rate of the surface potential decay can originate from the following reasons. Firstly, in the vicinity of the Si nanoparticles, the Coulomb interaction between electron and hole of the exciton is weakened due to the relative dielectric constant for silicon (12) is larger than for PVC (~3). This increases the probability of exciton decay into free charge carriers. Secondly, holes from the photoactive layer to the ITO electrode can transfer directly through the Si nanoparticles (Fig. 6). In addition, positions of the energy levels of the highest occupied molecular orbital (HOMO) of the organic molecules and the edge of the valence band of silicon shows the possibility of transferring holes from the photoconductor (PVC and CD) to PEDOT:PSS through Si nanoparticles with subsequent transfer to ITO. Nevertheless, the transfer through Si nanoparticles is more likely, since the mobility of holes in a Si crystal (~$10^2$ cm² V⁻¹ s⁻¹) is much greater than that in the PEDOT:PSS layer (~$10^{-5}$ cm² V⁻¹ s⁻¹ [11]).

## CONCLUSION

Using films of a photoconductive composite of PVC with a carbocyanine dye as an example, it is shown that adding a PEDOT:PSS hole transport layer between the photoconductor layer and the electrode increases the efficiency of hole transfer from the photoconductor to the electrode in the electrographic mode. This is a conventional approach for increasing the photoconductivity of organic electronic devices. We demonstrated that the introduction of silicon nanoparticles into the PEDOT:PSS layer further increases the hole transfer efficiency and the efficiency of the charge carrier photogeneration. In the work, to measure the surface potential, the electrographic method was modernized using a field-effect transistor in the electrometer, which increased the reliability of the measuring setup. The proposed approach of the EG method for determining the efficiency of photogeneration of charge carriers according to equation (1) makes it possible to improve the research and development of new photoconductive materials.

CONFLICT OF INTEREST

The authors declare that they have no conflicts of interest.

REFERENCES

1. E. L. Aleksandrova, Semiconductors **38**, 1115−1159 (2004).

2. P. M. Borsenberger and D. S. Weiss, *Organic Photo Receptors for Xerography* (Marcel Dekker, New York, 1999).

3. R. Osterbacka, K. Genevicius, A. Pivrikas, et al., Synth. Met. **139**, 811 (2003).
https://doi.org/10.1016/S0379-6779(03)00267-4

4. K. Ding, X. Huang, Y. Li, and S. R. Forrest, Energy Environ. Sci. **14**, 1584 (2021).
https://doi.org/10.1039/D0EE03885G

5. N. Kh. Ibrayev, D. A. Afanasyev, A. A. Ishchenko, and N. A. Davidenko, High Energy Chem. **47**, 41 (2013).
https://doi.org/10.1134/S0018143913020069

6. A. R. Tameev, L. Licea Jiménez, L. Ya. Pereshivko, et al., J. Phys.: Conf. Ser. **61**, **1152** (2007).
https://doi.org/10.1088/1742-6596/61/1/228

7. E. Ghavaminia, F. Behrouznejad, M. Forouzandeh, et al., RRL Solar **5**, 2100074 (2021).
https://doi.org/10.1002/solr.202100074

8. Y. Xu, Q. Niu, L. Zhang, et al., Polymers **14**, 2249 (2022).
https://doi.org/10.3390/polym14112249

9. K. A. Savin, P. A. Forsh, A. G. Kazansky, D. V. Amasev, A. R. Tameev, M. G. Tedoradze, D. E. Presnov, E. A. Forsh, V. A. Kulbachinsky, and P. K. Kashkarov, Nanotechnol. Russ. **15**, 770−777 (2020).
https://doi.org/10.1134/S1995078020060178

10. B. Fan, F. A. de Castro, J. Heier, et al., Org. Electron. **11**, 583 (2010).
https://doi.org/10.1016/j.orgel.2009.12.017

11. J. Niu, D. Yang, X. Ren, et al., Org. Electron. **48**, 165 (2017).
https://doi.org/10.1016/j.orgel.2017.05.044